Alternative Viterbi detection metrics for GFSK receivers: a hardware reduction approach

Jose Valencia-Velasco
Dept. of Electronics, Systems and IT
ITESO
Tlaquepaque, Mexico
ng100357@iteso.mx

Rodrigo Aldana-Lopez
Dept. of Electronics, Systems and IT
ITESO
Tlaquepaque, Mexico
raldanal@iteso.mx

Omar Longoria-Gandara
Dept. of Electronics,Systems and IT
ITESO
Tlaquepaque, Mexico
olongoria@iteso.mx

***Abstract*—Gaussian frequency shift keying (GFSK) is a digital modulation scheme with both attractive spectra and high power efficiencies. Modulation schemes with these characteristics often require a maximum likelihood sequence estimator (MLSE) implemented by means of Viterbi Algorithm (VA). The main drawback of VA is complexity implementation due to the filter bank needed to calculate the metrics, the large number of states required to describe the signal and the employment of squaring and multiplication operations in calculating metric cost.**

This paper discusses alternative metrics for VA in GFSK schemes that avoids the use of multiplication and squaring operations, achieving a reduction in implementation complexity. Moreover, the tradeoff between complexity and performance (in terms of bit error rate, BER) for the proposed metrics is shown under additive white Gaussian noise (AWGN).

***Index Terms*—digital modulation, continuous phase modulation (cpm), Viterbi decoding, reduced-complexity, IoT.**

I. Introduction

Gaussian frequency shift keying (GFSK) is an attractive digital modulation scheme, belonging to digital continuous phase modulation (CPM) schemes that exhibits high power and spectral efficiency with a constant envelope and a signal phase constrained to be continuous. Therefore, GFSK is used in many communication standards, e.g. Bluetooth low-energy (BLE) uses GFSK with frequency pulse shaping length $L = 3$ and a modulation index $h = 0.5$.

The optimal receiver for GFSK signaling consists of a matched filter bank followed by a Viterbi processor [1]. The matched filter bank is used to calculate a likelihood metric. Moreover, the amount of filters is proportional to the dimensionality of the signal space which may be large in different CPM formats [2].

In this sense, research works address the complexity problem related to the VA from two approaches: the first one is based in the reduction of the number of matched filters and the states required to describe the signal. The second approach is focused in the reduction of operations performed in the calculation of the metrics.

Regarding the first approach, in [3] is proposed a CPM receiver where the metric for VA is calculated using a linear approximation of the CPM signal. This results in a reduction in the number of matched filters and states required to describe the signal with a degradation of 0.24 dB, in the case of GMSK, with respect to the optimal receiver.

978-1-5386-6754-5/18/$31.00 ©2018 IEEE

In [4] it is demonstrated that four or six matched filters are sufficient to represent properly the reference signals if the CPM signal is approximated by a limited number of dimensions in the signal space per symbol interval. In addition, a reduction in the number of memory states is achieved by using reduced state sequence-detection algorithms. Results show a maximum loss in BER performance of 4.25 dB in a 4-ary CPM scheme with raised cosine (RC) frequency pulse. Another signal space reduction was developed in [5] resulting in a BER degradation in the order of 1 dB for a CPM signal with rectangular pulse shape

Moreover, in [6] and [7] propose a reduced complexity Viterbi detector, where the phase tree (the ensemble of all possible transmitted phase versus time functions) is approximated using a shorter frequency pulse. In this case, the BER degradation is 2.4 dB for a CPM modulation scheme with 4-RC.

Regarding the reduction of operations performed in the calculation of the metrics, in [8] the Euclidean metric is approximated with a series of linear functions, thus multiplications are replaced with digital left/right bit shifts and add operations resulting in a reduction of implementation complexity of VA.

In this paper, the reduced implementation complexity problem for GFSK demodulation in BLE receivers is addressed by quantizing the in-phase and quadrature components of the baseband signal, thereby the obtained values are $+1$ and -1. This quantized signal is used as input to the VA. Different modifications to the metric calculation are presented. Thus, the use of operations such as multiplications and squaring are avoided. In addition, simulations on additive white Gaussian noise (AWGN) channel for binary GFSK show the tradeoff between implementation complexity and performance using BER as a figure of merit. Simulation results show a loss in performance, but requirements for BLE standard are compliant.

The rest of this paper is organized as follows. Section II presents the system model, while in Section III the proposed metrics for the Viterbi processor are described. In Section IV the simulated performance in terms of BER is shown

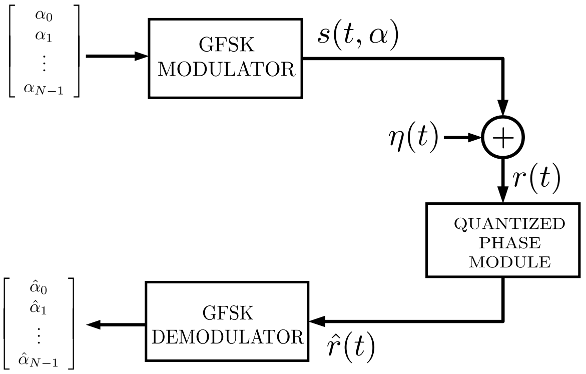

Fig. 1. General block diagram of a GFSK communication system.

and the tradeoff between complexity and BER performance is analyzed. Finally, in Section V conclusions are drawn.

II. Signal Model

Figure 1 shows the general block diagram of a GFKS communication system. The first part consist of a GFSK modulator which takes the input string of N symbols $\boldsymbol{\alpha} = \alpha_0, \alpha_1, \alpha_2, \ldots, \alpha_{N-1}$ and generates the complex envelope of a GFSK signal that is described as follows:

$$s(t,\boldsymbol{\alpha}) = \exp\{j\phi(t,\boldsymbol{\alpha})\} \tag{1}$$

with the following definitions:

$$\phi(t,\boldsymbol{\alpha}) = 2\pi h \sum_{i=0}^{k} \alpha_i q(t-iT) \tag{2}$$

$$\alpha_i \in \{+1,-1\} \qquad kT \leq t < (k+1)T$$

where the modulation index is represented by h and T is the symbol interval. The phase response, $q(t)$, related to the Gaussian pulse shaping $g(t)$, with a duration of L symbol periods, is described as

$$q(t) = \int_0^t g(\tau)d\tau \tag{3}$$

with

$$\begin{aligned} g(t) = \quad & \tfrac{1}{2T}\left[Q\left(2\pi BT\left(\tfrac{t-T/2}{\sqrt{\ln(2)}T}\right)\right)\right. \\ & \left. -Q\left(2\pi BT\left(\tfrac{t+T/2}{\sqrt{\ln(2)}T}\right)\right)\right] \end{aligned} \tag{4}$$

where Q is the complementary error function.

The function $q(t)$ has a maximum value of $1/2$ for $t > L$. These maximum values are accumulated over time, thus $\phi(t,\boldsymbol{\alpha})$ can be written as

$$\begin{aligned} \phi(t,\boldsymbol{\alpha}) &= 2\pi h \sum_{i=k-L+1}^{k} \alpha_i q(t-iT) + \pi h \sum_{i=0}^{k-L} \alpha_i \bmod 2\pi \\ &= \theta(t,\alpha_k,\ldots,\alpha_{k-L+1}) + \theta_k \qquad kT \leq t < (k+1)T \end{aligned} \tag{5}$$

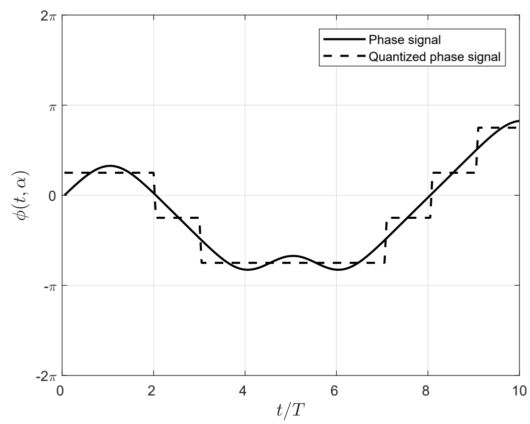

Fig. 2. Continuous and quantized phase signal for the symbols $\{-1,-1,-1,-1,1,1,1,-1\}$ using GFSK.

where $\theta(t,\alpha_k,\ldots,\alpha_{k-L+1})$ is the phase contribution between time $(k-L+1)T$ and t, and θ_k represents the phase accumulation up to time $(k-L+1)T$.

In the case of GFSK, with $h = 0.5$, $BT = 0.3$ and a partial response of $L = 3$, the complex envelope signal results in:

$$\begin{aligned} s(t,\boldsymbol{\alpha}) &= \exp\{\pi j(\alpha_k q(t-kT)+ \\ \alpha_{k-1}q(t-(k-1)T) &+ \alpha_{k-2}q(t-(k-2)T) + j\theta_k\} \end{aligned} \tag{6}$$

It is assumed that the signal is transmitted over a Gaussian channel. The baseband received signal, $r(t,\boldsymbol{\alpha})$, is described as

$$r(t) = s(t,\boldsymbol{\alpha}) + \eta(t) \tag{7}$$

where $\eta(t)$ is a zero-mean additive complex white Gaussian noise with variance $\sigma^2 = N_0/2$ per real and imaginary components and power spectral density of $N_0/2$.

III. Receiver design

In this section a particular case of receiver is analyzed. The following receiver starts with a quantized phase module with the advantage of simplifying the hardware implementation of the detection algorithms.

A. Quantized phase module

In this section, a quantization of the received signal phase is studied. Taking the signal from (5), let the uniform quantization of $\phi(t,\boldsymbol{\alpha})$ with step size $\pi/2$ and offset $\pi/4$ be:

$$\hat{\phi}(t,\boldsymbol{\alpha}) = \frac{\pi}{2}\left\lfloor \frac{2}{\pi}\phi(t,\boldsymbol{\alpha}) \right\rfloor + \frac{\pi}{4} \tag{8}$$

where $\lfloor\cdot\rfloor$ is the floor operation. An example of this quantized phase is shown in Fig. 2.

Furthermore, the following identitiy can be verified:

$$\sqrt{2}|\cos(\hat{\phi}(t,\boldsymbol{\alpha}))| = \sqrt{2}|\sin(\hat{\phi}(t,\boldsymbol{\alpha}))| = 1 \tag{9}$$

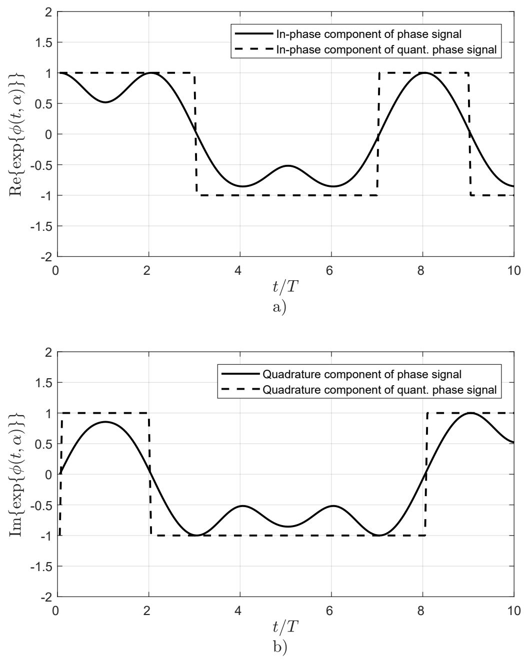

Fig. 3. Complex envelope components for the continuous and quantized phase signal usign GFSK. a) In-phase component, b) Quadrature component.

Therefore,

$$\mathrm{sign}(\cos(\phi(t,\boldsymbol{\alpha}))) = \mathrm{sign}(\cos(\hat{\phi}(t,\boldsymbol{\alpha}))) = \sqrt{2}\cos(\hat{\phi}(t,\boldsymbol{\alpha})) \tag{10}$$

and

$$\mathrm{sign}(\sin(\phi(t,\boldsymbol{\alpha}))) = \mathrm{sign}(\sin(\hat{\phi}(t,\boldsymbol{\alpha}))) = \sqrt{2}\sin(\hat{\phi}(t,\boldsymbol{\alpha})) \tag{11}$$

where

$$\mathrm{sign}(x) = \begin{cases} +1 & \text{if} \quad x \geq 0 \\ -1 & \text{if} \quad x < 0 \end{cases} \tag{12}$$

Using these results, the corresponding baseband signal to the quantized phase signal is constructed as:

$$\hat{s}(t,\boldsymbol{\alpha}) = \sqrt{2}\exp\{j\hat{\phi}(t,\boldsymbol{\alpha})\} = \tag{13}$$
$$\mathrm{sign}(\cos(\phi(t,\boldsymbol{\alpha}))) + j\mathrm{sign}(\sin(\phi(t,\boldsymbol{\alpha})))$$

Such description of the received signal is convenient since it can be represented using only ± 1 instead of an infinite number of values in the interval $[-1, 1]$. An example of this signal is depicted in Fig. 3. This can be used to find simplified hardware implementations for detection algorithms.

Applying the described quantization process to the received signal (7), it yields:

$$\hat{r}(t) = \mathrm{sign}(\mathrm{Re}\{r(t)\}) + j\mathrm{sign}(\mathrm{Im}\{r(t)\}) \tag{14}$$

B. Trellis diagram for the quantized phase signal

The GFSK signal (6) is given by the transmitted symbol α_k, the correlative state vector $(\alpha_{k-1}, \alpha_{k-2})$ and the phase memory θ_k. Thus, it can be represented by the total state vector $\sigma_k = (\theta_k, \alpha_{k-1}, \alpha_{k-2})^T$ and the symbol α_k. Let the phase reference signal in the receiver

$$\Phi(t,\alpha_k,\sigma_k) = \pi(\alpha_k q(t-kT) + \alpha_{k-1}q(t-(k-1)T) \tag{15}$$
$$+\alpha_{k-2}q(t-(k-2)T) + \theta_k.$$

The transition rule of the total state vector σ_k over the time intervals can be represented by the following vector:

$$\sigma_{k+1} = \begin{pmatrix} 1 & 0 & \pi/2 \\ 0 & 0 & 0 \\ 0 & 1 & 0 \end{pmatrix} \sigma_k + \begin{pmatrix} 0 \\ 1 \\ 0 \end{pmatrix} \alpha_k \tag{16}$$

Note that since θ_k can only take values in $\{0, \pi/2, \pi, 3\pi/2\}$ for $h = 0.5$, hence there are 16 possible combinations for σ_k. Therefore, the trellis diagram can be constructed using the possible states σ_k and the transition rule (16) as shown in Fig. 4. The trellis diagram is extended for T_b intervals, where T_b is known as the traceback, so that the goal is to estimate the sequence $\alpha_k, \ldots, \alpha_{k+T_b-1}$. A well known estimation algorithm is the Viterbi Algorithm [9], which obtains the maximum likelihood sequence estimation (MLSE). The received signal is compared with a reference signal in a certain path along the trellis using a likelihood metric. The MLSE is chosen to be the path with the best metric value. Ideally, the traceback value would be large enough to cover the entire received sequence. In practice, an heuristic is applied and T_b can be reduced up to

$$T_b = 5\log_2(Q) \tag{17}$$

where $Q = 16$ is the number of possible states in the trellis diagram.

C. Traditional metric

Traditionally, the metric used in the Viterbi algorithm for CPM signals, is calculated as the Euclidean distance between the received signal $r(t)$ and the reference signal in the state σ_k and α_k:

$$J_k(\alpha_k,\sigma_k) = \int_{kT}^{(k+1)T} \|r(t) - S(t,\alpha_k,\sigma_k)\|^2 dt \tag{18}$$

where

$$S(t,\alpha_k,\sigma_k) = \exp(j\Phi(t,\alpha_k,\sigma_k)) \tag{19}$$

is the reference signal. A discrete-time version of this metric can be written as:

$$J_k(\alpha_k,\sigma_k) = \sum_{n=M_p k}^{M_p(k+1)-1} \|r(n) - S(n,\alpha_k,\sigma_k)\|^2 \tag{20}$$

where the time has been over-sampled by a factor of M_p samples per symbol period. Note that this approach requires storing all the reference sequences $S(n,\alpha_k,\sigma_k)$ in memory in order to compute the MLSE path. Furthermore, it requires these samples to be represented with a given precision which can be called a single *word* without loss of generality. The size of the word defines the size of the adders, subtractors and multipliers required to implement (20).

D. Metric proposal 1

Taking the traditional approach as a reference, the quantized phase signal $\hat{r}(t)$ can be compared directly with the reference signals using an Euclidean distance as:

$$J_k(\alpha_k,\sigma_k) = \int_{kT}^{(k+1)T} \|\hat{r}(t) - S(t,\alpha_k,\sigma_k)\|^2 dt \qquad (21)$$

A discrete-time version of (21) can be written as:

$$J_k(\alpha_k,\sigma_k) = \sum_{n=M_p k}^{M_p(k+1)-1} \|\hat{r}(n) - S(n,\alpha_k,\sigma_k)\|^2 \qquad (22)$$

This approach is simpler than the traditional approach since the real and imaginary parts of the signal $\hat{r}(n)$ can only be 1 or -1. Therefore, in order to compute (22) is enough to store the pre-computed signals:

$$\begin{aligned} D_1(n,\alpha_k,\sigma_k) &= \|(1+j) - S(n,\alpha_k,\sigma_k)\|^2 \\ D_2(n,\alpha_k,\sigma_k) &= \|(-1+j) - S(n,\alpha_k,\sigma_k)\|^2 \\ D_3(n,\alpha_k,\sigma_k) &= \|(1-j) - S(n,\alpha_k,\sigma_k)\|^2 \\ D_4(n,\alpha_k,\sigma_k) &= \|(-1-j) - S(n,\alpha_k,\sigma_k)\|^2 \end{aligned} \qquad (23)$$

with a precision word per sample. Then, a sample of one of these signals is selected depending on the signs of the real and imaginary part of $\hat{r}(n)$. This saves the multipliers and the subtractors, leaving only the word-sized adders, but with 4 times the required memory with respect to the traditional approach.

E. Metric proposal 2

Another possible metric is to compare $\hat{r}(n)$ with a quantized phase version of the reference signals $\hat{S}(t,\alpha_k,\sigma_k)$:

$$J_k(\alpha_k,\sigma_k) = \frac{1}{4}\int_{kT}^{(k+1)T} \|\hat{r}(t) - \hat{S}(t,\alpha_k,\sigma_k)\|^2 dt \qquad (24)$$

A discrete-time version of (24) can be written as:

$$J_k(\alpha_k,\sigma_k) = \frac{1}{4}\sum_{n=M_p k}^{M_p(k+1)-1} \|\hat{r}(n) - \hat{S}(n,\alpha_k,\sigma_k)\|^2 \qquad (25)$$

This simplifies the required precision for the samples, since both $\hat{r}(n)$ and $\hat{S}(n,\alpha_k,\sigma_k)$ can be represented using just 2 bits each. For instance, let $\{r_R\ r_I\}$ represent $\hat{r}(n)$ and $\{S_R\ S_I\}$ represent $\hat{S}(n,\alpha_k,\sigma_k)$ e.g. $\{r_R\ r_I\} = \{0\ 1\}$ corresponds to $\hat{r}(n) = 1-j$. Furthermore, the result of $\|\hat{r}(n)-\hat{S}(n,\alpha_k,\sigma_k)\|^2$ can only be $0, 1$ or 2 and is represented using 2 bits as well $\{J_1\ J_2\}$, where $\{0\ 0\}$ corresponds to 0, $\{0\ 1\}$ to 1 and $\{1\ 0\}$ to 2. The relationship between $\{r_R\ r_I\ S_R\ S_I\}$ and $\{J_1\ J_2\}$ can be expressed as a look up table or as the boolean equations:

$$\begin{aligned} J_2 &= (r_R \oplus S_R) \oplus (r_I \oplus S_I) \\ J_1 &= (r_R \oplus S_R) \cdot (r_I \oplus S_I) \end{aligned} \qquad (26)$$

TABLE I
COMPARISON OF HARDWARE RESOURCES BETWEEN THE PROPOSED METRICS

Metric	Bus size	Adders	Subs.	Mult.	Memory
Trad.	1 word	$M_p - 1$	M_p	M_p	$2QM_p$ words
Prop. 1	1 word	$M_p - 1$	0	0	$8QM_p$ words
Prop. 2	$2 + \log_2(M_p)$ bits	$M_p - 1$	0	0	$4Q$ bits

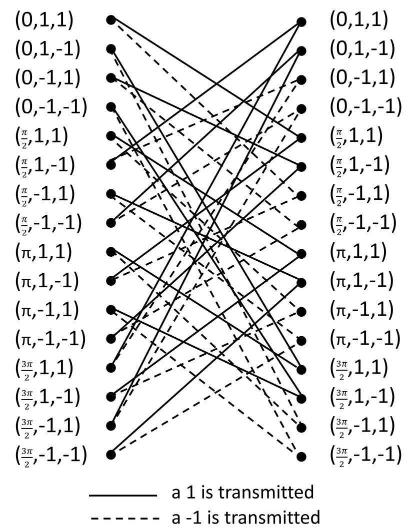

Fig. 4. Trellis diagram for a GFSK signal with modulation index of 0.5 and pulse lenght of 3 symbol periods.

These bits are used to select if $0, 1$ or 2 is added to the metric calculation (25). Moreover, the amount of memory is reduced since only two bits are needed to store $\hat{S}(n,\alpha_k,\sigma_k)$, resulting in a total of $2(2Q)$ considering all states. Furthermore, the adder bus size is simplified since in the worst case the metric results in $2M_p$ which require $2+\log_2(M_p)$ to be represented.

Note that this metric turns out equivalent to the following metric:

$$\begin{aligned} J_k(\alpha_k,\sigma_k) &= H_k(\mathrm{Re}\{\hat{r}(n)\}, \mathrm{Re}\{\hat{S}(n,\alpha_k,\sigma_k)\}) \\ &+ H_k(\mathrm{Im}\{\hat{r}(n)\}, \mathrm{Im}\{\hat{S}(n,\alpha_k,\sigma_k)\}) \end{aligned} \qquad (27)$$

Where $H_k(\cdot,\cdot)$ is the Hamming distance operation for signals with range $\{1,-1\}$ and can be computed as

$$H_k(x(n),y(n)) = \frac{1}{2}\sum_{n=M_p k}^{M_p(k+1)-1} |x(n) - y(n)| \qquad (28)$$

which counts the amount of different samples between $x(n)$ and $y(n)$ in the interval $[M_p k, M_p(k+1)-1]$ [10].

A summary of the usage of hardware resources is shown in Table I.

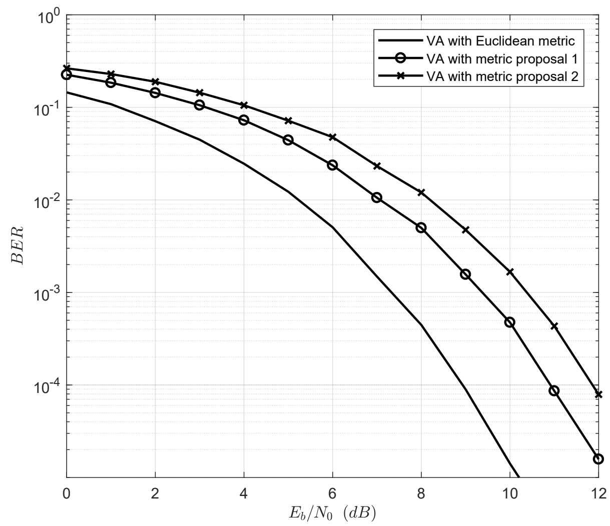

Fig. 5. BER performance of GFSK VA using the Euclidean and the proposed metrics.

IV. Simulation Results

This section presents simulation results of the proposed metrics for VA taking BER performance as the figure of merit. The simulation scenario is represented in Fig. 1. It uses the baseband modulator described in (1) and the demodulator with the metrics detailed in Section III. The transmission consisted of 10^7 symbols, in order to achieve a BER performance of 10^{-5}, for E_b/N_o values of 0 to 12 dB. Furthermore, the BER of GFSK using VA with traditional metric is used as a BER lower boundary. An AWGN channel with a zero mean is considered.

The modulators were configured with the following parameters: $BT = 0.5$, a pulse $g(t)$ with $L = 3$ symbol periods and $h = 0.5$. The GFSK Viterbi parameters considered were: pulse length of 3 symbol periods, $BT = 0.5$ and a traceback of 20 symbol periods.

Figure 5 shows the BER performance of the VA with the metrics described in (22) and (25). In addition, the BER performance of GFSK Viterbi with traditional metric is included. Note that the performance of the proposals meets the specification for the BLE standard (BER of 0.1% at SNR of 21 dB) considering $h = 0.5$. Furthermore, it can be observed that metric proposal 1 outperforms proposal 2 with a gain of 1 dB, and it presents a loss of 2 dB when compared to the VA with traditional metric for a BER of 10^{-3}. These results show that there is a tradeoff between the hardware resources reduction, shown in Table I, and the performance in terms of BER. However, this tradeoff can be balanced by means of comparing the huge saving in hardware resources since no multipliers are used and reduced adders are included.

V. Conclusions

In this paper are proposed alternative metrics for GFSK receivers based in VA that can be used in Bluetooth receivers for IoT technologies. A detailed analysis for each metric, considering a modulation index of 0.5, is revised and the hardware resource usage is determined. The complexity of the receivers that use the proposed metrics is reduced due to the quantization of the received and reference signals, allowing its in-phase and quadrature branches be represented with only two values, implying a simplification in the calculus of the metric since no multiplications or squaring operations are required. Simulation results show a loss in BER performance of 2 dB and 3 dB for metric proposal 1 and 2, respectively, when they are compared to the traditional Viterbi decoder. The proposed metrics have the advantage of having considerably lower hardware resources than the traditional approach, still compliant with BLE standard BER requirements.

References

[1] J.G. Proakis, *Digital communications*. San Diego, CA: Mc Graw Hill, 2001.

[2] U. Mengali and M. Morelli, "Decomposition of M-ary CPM signals into PAM waveforms," *IEEE Transactions on Information Theory*, vol. 41, pp. 1265–1275, Sep. 1995.

[3] G. K. Kaleh, "Simple coherent receivers for partial response continuous phase modulation," *IEEE Journal on Selected Areas in Communications*, vol. 7, no. 9, pp. 1427–1436, Dec. 1989.

[4] J. Huber and W. Liu, "An alternative approach to reduced-complexity CPM-receivers," *IEEE Journal on Selected Areas in Communications*, vol. 7, no. 9, pp. 1437–1449, Dec. 1989.

[5] T. Palenius and A. Svensson, "Reduced complexity detectors for continuous phase modulation based on a signal space approach," *European Transactions on Telecommunications*, vol. 4, no. 3, pp. 285–297, Jun. 1993.

[6] Svensson Arne, Aulin Tor, Sundberg Carl, "A class of reduced-complexity Viterbi detectors for partial response continuous phase modulation," *IEEE Transactions on Communications*, vol. 32, Oct. 1984.

[7] A. T. Anderson John and S. Carl, *Digital phase modulation*. New York, USA: Springer Science & Business Media, 1986.

[8] C. R. Zayed Nick M., "Generalized partial response signalling and efficient MLSD using linear Viterbi branch metrics," Dec. 1999.

[9] G. D. Forney, "The Viterbi algorithm," *Proceedings of the IEEE*, vol. 61, no. 3, pp. 268–278, Mar. 1973.

[10] D. J. S. Robinson, *An Introduction to Abstract Algebra*. Illinois, USA: Walter de Gruyter, Jan. 2003.